DELAY LINE WITH DIFFERENT RECEIVER-RESONATOR CHANNELS AS AN ALL MECHANICAL FRONT-END OF A DISCRETE MATCHED FILTER FOR WAKE-UP RADIOS

Gabriel Vidal-Álvarez, Abhay Kochhar, and Gianluca Piazza
Carnegie Mellon University, Pittsburgh, USA

ABSTRACT

We present the conceptual approach, theoretical simulations, and experimental results of a new radio frequency mechanical signal processor composed of a delay line with one transmitter and several receivers integrated with resonators. The system allows to set different delays and voltage gains for every receiver-resonator subsystem (channel), hence enabling processing of discrete chirp signals or complex frequency-shift keying (FSK) signals. We show results for a 2-channel system. The experimental results show voltage gain and different delay for each channel. This all-mechanical signal processor is ideal for improving signal-to-noise ratio in low-power wake-up radio receivers.

INTRODUCTION

There is an ongoing effort to improve the limit of detection and power consumption of wake-up radios [1], [2]. Recent work has shown detection of signals as low as $-69\ dBm$ with $< 10\ nW$ of power consumption [3], [4]. However, these approaches use only a single frequency, which is ultimately not appropriate to meet the signal capacity and signal-to-noise ratio (SNR) required for large sensor networks. Ultimately, the use of a single frequency also makes the individual wake-up receiver more prone to detect false events. Having a broadband or multi-frequency receiver greatly mitigates this problem. Our proposed approach is based on implementing the front-end of a discrete matched filter using all passive micromechanical components formed by delay lines and resonators.

A challenge in the implementation of this system is in the realization of delay lines with sufficiently long delays (τ), minimal losses, and wide bandwidth. Similarly, high voltage gains (G) given a capacitive load (representative of the input impedance of a MEMS demodulator [5]) are only possible when very high electromechanical coupling ($k_t{}^2$) resonators are available [6]. The use of suspended films of X-cut lithium niobate ($LiNbO_3$, dubbed LN) with very low stress enables synthesizing delays in excess of $1\ \mu s$ and simultaneously harness the large coupling coefficients to attain a wideband operation with low loss [7]. The high $k_t{}^2$ in conjunction with high quality factor (Q) permits achieving high voltage gains in compact laterally vibrating resonators [8].

MATCHED FILTER OVERVIEW

We present a new system comprised of an acoustic delay line with one transmitter and several receivers, each one connected to an acoustic resonator (Figure 1). The transmitter, formed by an interdigitated transducer (IDT) patterned on LN, is broadband, *i.e.* it is able to launch an acoustic wave over a broad

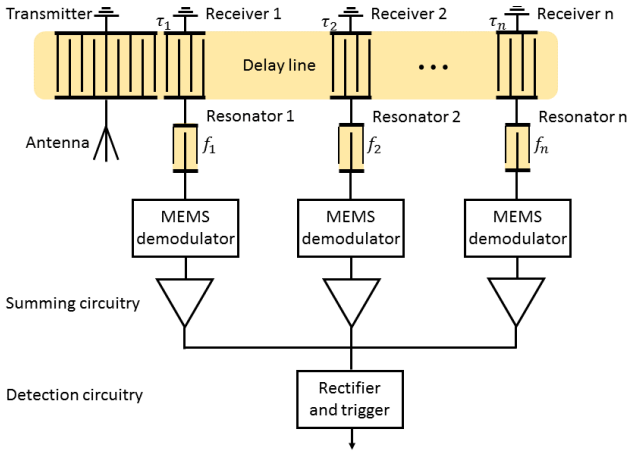

Figure 1: Schematic of the proposed wake-up radio receiver composed of a discrete matched filter with an arbitrary number of channels n and the detection circuitry. The front-end of the matched filter is the part that we present in this work (color background). It is composed of a delay line with several receivers connected to different resonators. The separation between transmitter and receiver sets the delay of the channel. The resonator with an attached capacitive load sets the frequency and voltage gain of the channel (the demodulator can be modeled as an equivalent capacitive load at the RF frequency of the resonator [5]). The rest of the wake-up receiver is presented through block diagrams of the various components. It is comprised of MEMS demodulators to down convert the RF signal of every channel and of CMOS circuitry to collect the signal from the different channels and amplify it. This latter part compose the back-end of the matched filter. Finally, there is the CMOS detection circuitry that is used to trigger a wake-up signal.

spectrum of frequencies around a central frequency. Each receiver, formed as well by an IDT, is connected to a high Q resonator, making the receiver-resonator subsystem narrowband, *i.e.* each element of the subsystem is tuned to detect a single frequency.

Every receiver-resonator subsystem forms what we call a channel. The position of the receiver in the delay line sets the delay of the channel. The resonator acts as a narrowband filter setting the frequency of the channel. Additionally, the resonator provides for voltage gain (defined as the ratio of the voltage on the capacitor to the voltage provided by the voltage source) when terminated with a capacitive load [6]. The input transducer of the delay line (transmitter) can be sized to ensure matching to a $50\ \Omega$ input. The receiver transducers and resonators of every channel can all be sized to maximize voltage gain for a given capacitive load.

DEVICE FABRICATION

The delay line is made of a plate of X-cut lithium niobate with interdigital transducers placed at different locations. One of the IDTs acts as a transmitter launching the acoustic signal. The other IDTs act as receivers picking up the acoustic signal sent by the transmitter.

The resonators are also made of a plate of X-cut lithium niobate with an IDT on top. However, in the case of the resonators, the lithium niobate plate edges are etched so as to form a resonant cavity.

The delay line and resonators are fabricated within the same process. We fabricate them in a 1 μm X-cut lithium niobate thin film provided by NGK Insulators. We orient both the delay line and resonators at 30° with respect to the Y axis of the LN wafer. This orientation maximizes the coupling coefficient for propagation of the S_0 mode in both delay line and resonators. For more details on the fabrication process see reference [7]. Figure 2 shows an optical image of the full system: the delay line with a single transmitter and the different receivers with connected resonators.

EXPERIMENTAL RESULTS

We report experimental results for the 2-channel system shown in Figure 2. This device was designed with the following geometrical parameters:

- Transmitter: pitch of 9 μm ($\lambda_T = 18\,\mu m$) to operate around 330 MHz, electrode coverage of $2w_{f_T}/\lambda_T = 1/3$, number of fingers $N_T = 40$, and aperture $l_{DL} = 175.5\,\mu m$. With these parameters, the transmitter presents an equivalent impedance close to 50 Ω at the maximum transmission of the passband.
- Receivers: identical to the transmitter.
- Delay: gap between transmitter and receiver of $l_{g_1} = 80\lambda_T$ for channel 1 and of $l_{g_2} = 180\lambda_T$ for channel 2.
- Resonators: wavelength is $\lambda_{R_1} = 18\,\mu m$ for channel 1 and $\lambda_{R_2} = 17.925\,\mu m$ for channel 2, electrode coverage $2w_{f_{R_{1,2}}}/\lambda_{R_{1,2}} = 1/3$, number of fingers $N_{R_{1,2}} = 21$ (counting the two reflectors at the edges of the resonator as fingers [9]), and aperture $l_{R_{1,2}} = 11.5\lambda_{R_{1,2}}$. These parameters were selected so that the static capacitance of the resonators ($240\ fF$) provides for a voltage gain close to its maximum for a fixed capacitive load of 300 fF (see results for a standalone resonator in [10]).

We performed electrical measurements of the system with a network analyzer. We use the measured results and virtually terminate them with a capacitive load of 300 fF to investigate the available voltage gains. Figure 3 shows the voltage gain and group delay for channel 1. Figure 4 shows the same variables for channel 2. By comparing the two figures, it is clear that the gain and group delay are different for the two channels. The different delays are due to the different position of the receivers in the delay line. It is important to note that the total group delay values do not only account for the delay in the delay line but also include the delay from the resonators. Only the relative delay (the relevant one in a matched filter) between the channels is due to the different placement of the receivers. The difference in gain between the two channels is discussed in the next section. Figure 3 and Figure 5 show additional peaks surrounding the main one. These peaks are due to spurious resonances in the delay line due to the in-line nature of the IDTs [11].

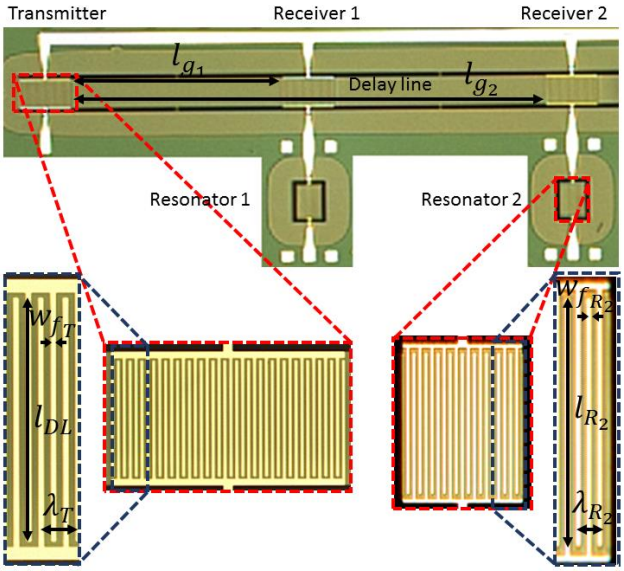

Figure 2: Optical image of a fabricated 2-channel system. The different paramaters labeled for an IDT (either of delay line or resonator) are: wavelength λ, finger widht w_f, and aperture l. The channel delay (transmitter-receiver gap) l_g is also labeled.

DISCUSSION

Figure 5 shows the expected voltage gain for the fabricated system. The theoretical results are based on both lumped element as well as distributed element models for the delay line and the resonators [12], [13]. To calculate every component of both models we use the following parameters:

- Lithium niobate: mass density $\rho = 4700\ kg/m^3$, relative permittivity $\varepsilon_r = 40$, phase velocity $v = 7000\ m/s$ for the distributed element model and $v = 6000\ m/s$ for the lumped element model (we use two different values because the two models use different definitions of phase velocity), piezoelectric coefficient e along the direction of propagation of $e = -4.65\ C/m^2$ which is equivalent to an electromechanical coupling of ${k_t}^2 = 32\%$, and propagation loss $\alpha = 15\ dB/cm$ which is equivalent to a quality factor $Q = 1000$ for the lumped Butterworth van Dike (BVD) resonator model.
- Transmitter: electromechanical coupling ${k_t}^2 = 60\%$ (a higher value than the one corresponding to the intrinsic coupling in the material was used to fit for the maximum transmission of the transmitter. This approach is a clear approximation as it fails to fit the asymmetric response of an in-line IDT using a lumped element model IDT that has a symmetric response).
- Receivers: same electromechanical coupling of transmitter.
- Resonators: electromechanical coupling ${k_t}^2 = 25\%$ (a slightly lower value than the maximum intrinsic value for this mode of vibration based on the response of similar devices in the same fabrication process).

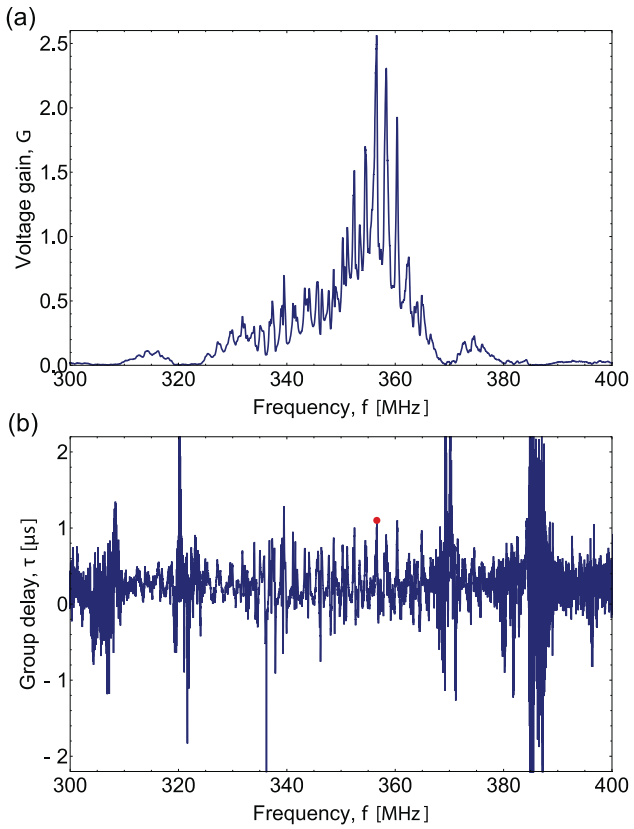

Figure 3: Voltage gain and group delay for channel 1 obtained from the experimental results when resonator 1 is virtually terminated with a 300 fF capacitive load. (a) Voltage gain. (b) Group delay. The red dot indicates the group delay at the frequency of maximum gain.

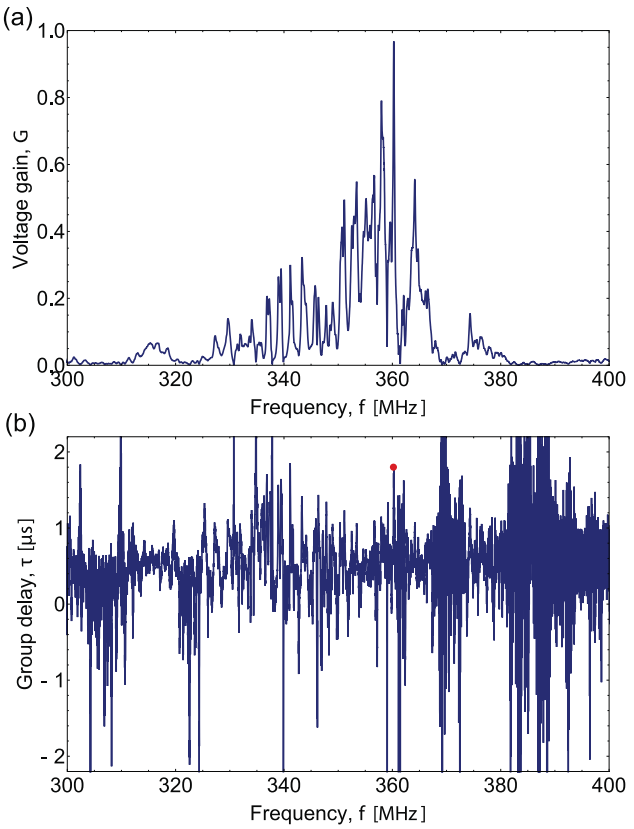

Figure 4: Voltage gain and group delay for channel 2 obtained from the experimental results when resonator 2 is virtually terminated with a 300 fF capacitive load. (a) Voltage gain. (b) Group delay. The red dot indicates the group delay at the frequency of maximum gain.

The experimental and theoretical results show good agreement. The lumped element model is faster to compute and therefore it is ideal to rapidly investigate the design space. The distributed element model describes more accurately the response of the system since it also considers the reflections coming from the in-line IDTs in the delay line.

We investigate the dependence of the voltage gain of a channel on the wavelength of the resonator relative to the receiver. We use channel 1 as an example for the study and vary the wavelength of resonator 1 while keeping the transmitter, delay, and receiver fixed. Figure 6 shows the change in voltage gain when the resonator wavelength ranges from $\lambda_{R_1} = 12\,\mu m$ to $\lambda_{R_1} = 24\,\mu m$. We see that the gain versus resonator wavelength follows closely the transfer function of the transmitter-receiver system. However, note that the curve is slightly shifted to longer wavelengths, *i.e.* it is not centered around $\lambda_{R_1} = 18\,\mu m$, but around $\lambda_{R_1} = 19\,\mu m$. This is because the frequency of operation of the resonator is shifted due to the capacitive load as well as the susceptance of the receiver.

From Figure 5 and Figure *6* we note that the fabricated resonators do not have the appropriate wavelength to maximize the voltage gain. The wavelengths of the resonators forming channel 1 and 2 are far from the range that gives maximum voltage gain. In addition, because of their relative position, they offer quite different gains. This explains the difference in voltage gain between the two channels in addition to any propagation loss coming from the different distance between transmitter and receiver for the two channels. Therefore, the matched filter response can be significantly improved by changing the center frequency of the two resonators.

CONCLUSIONS

We fabricated on a thin film of X-cut lithium niobate a delay line with one transmitter and two channels (receiver connected to a resonator) as the front-end of a discrete matched filter. We showed experimental results of a fabricated device. The results show different delays and gains for the two channels. We modeled a channel with lumped and distributed element models and studied theoretically the gain of the channel when terminated with a capacitive load, representative of a mechanical demodulator. The results agree well with theory and lay the foundation for the development of novel all-mechanical front-ends for processing very low power signals.

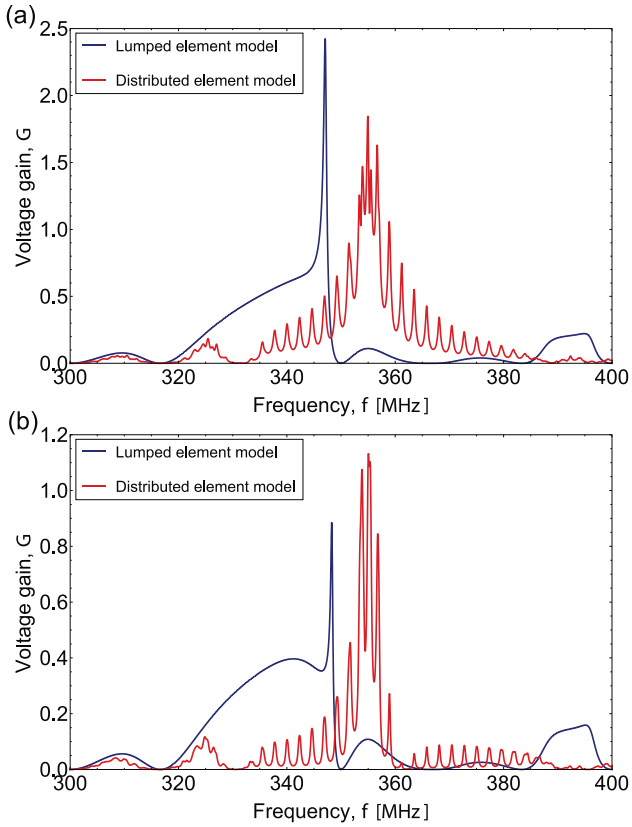

Figure 5: Theoretical voltage gain for the two channels when terminated with a 300 fF capacitive load. The theoretical results are obtained with both lumped element and distributed element models. (a) Voltage gain for channel 1. (b) Voltage gain for channel 2.

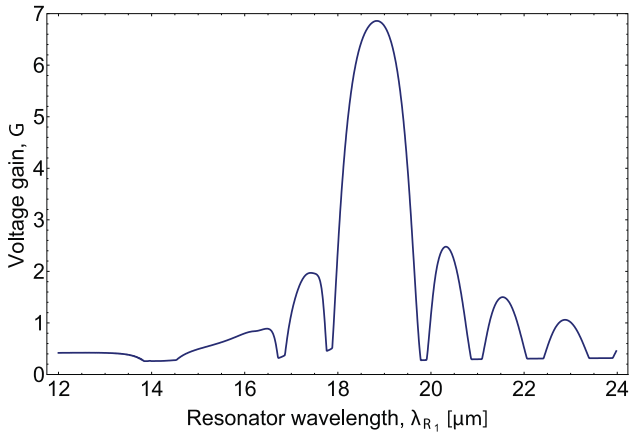

Figure 6: Theoretical voltage gain versus resonator wavelength for channel 1 terminated with a load of 300 fF.

ACKNOWLEDGEMENTS

The material presented is based upon work supported by the Defense Advanced Research Projects Agency (DARPA) under Contract No. HR0011-15-C-0137. Any opinions, findings, and conclusions or recommendations expressed in this publication are those of the author(s) and do not necessarily reflect the views of DARPA.

REFERENCES

[1] D. D. Wentzloff, "Low Power Radio Survey," online, www.eecs.umich.edu/wics/low_power_radio_survey.html

[2] J. Blanckenstein, J. Klaue, and H. Karl, "A Survey of Low-Power Transceivers and Their Applications," *IEEE Circuits and Systems Magazine*, vol. 15, no. 3, pp. 6–17, 2015.

[3] H. Jiang, et al., "A 4.5 nW wake-up radio with -69 dBm Sensitivity," presented at 2017 IEEE International Solid-State Circuits Conference (ISSCC), pp. 416–417, 2017.

[4] P. P. Wang, et al., "A 400 MHz 4.5 nW -63.8 dBm Sensitivity Wake-Up Receiver Employing an Active Pseudo-Balun Envelope Detector," presented at 43rd IEEE European Solid State Circuits Conference (ESSCIRC), pp. 1–4, 2017.

[5] M. E. Galanko, et al., "CMOS-MEMS resonant demodulator for near-zero-power RF wake-up receiver," presented at the 19th International Conference on Solid-State Sensors, Actuators, and Microsystems (TRANSDUCERS), pp. 86–89, 2017.

[6] R. Lu, et al., "Piezoelectric RF resonant voltage amplifiers for IoT applications," presented at the 2016 IEEE/MTT-S International Microwave Symposium (MTT), pp. 1–4, 2016.

[7] G. Vidal-Álvarez, A. S. Kochhar, and G. Piazza, "Delay Lines Based on a Suspended Thin Film of X- Cut Lithium Niobate," presented at the 2017 International Ultrasonics Symposium (IUS), pp. 1–4, 2017.

[8] F. V. Pop, et al., "Laterally vibrating lithium niobate MEMS resonators with 30% electromechanical coupling coefficient," presented at the 30th International Conference on Micro Electro Mechanical Systems (MEMS), pp. 966-969, 2017.

[9] S. Gong and G. Piazza, "Figure-of-Merit Enhancement for Laterally Vibrating Lithium Niobate MEMS Resonators," *IEEE Transactions on Electron Devices*, vol. 60, no. 11, pp. 3888–3894, 2013.

[10] L. Colombo, et al., "Ultra-Low-Power and High Sensitivity Resonant Micromechanical Receiver," presented at the 2017 IEEE Sensors, 2017.

[11] T. W. Bristol, et al., "Applications of Double Electrodes in Acoustic Surface Wave Device Design," presented at the 1972 Ultrasonics Symposium, pp. 343–345, 1972.

[12] D. P. Morgan, *Surface-wave Devices for Signal Processing*. North-Holland, 1991.

[13] S. Datta, *Surface acoustic wave devices*. Prentice Hall, 1986.

CONTACT

*G. Vidal-Álvarez, gvidal@andrew.cmu.edu